Applied Energy 399 (2025) 126492

Contents lists available at ScienceDirect

Applied Energy

journal homepage: www.elsevier.com/locate/apen

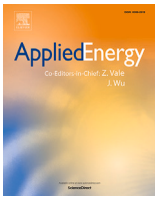

Modeling battery aging in linear energy system optimizations by applying convex hulls - accuracy benefits and computational costs

Petrin Geert Kristian*, Arens Stefan, Schoenfeld Patrik, Klement Peter, Schlüters Sunke

DLR Institute for Networked Energy Systems, Carl-von-Ossietzky-Straße 15, Oldenburg, 26129, Lower Saxony, Germany

HIGHLIGHTS

- Integration of accurate battery aging into linear optimization.
- Aging model including calendric and cyclic aging.
- Application: overhead line island buffer storage.
- Up to 46.9 % lower battery aging due to optimized operation.
- Omission of mixed integer linear programming, thus low computational costs.

GRAPHICAL ABSTRACT

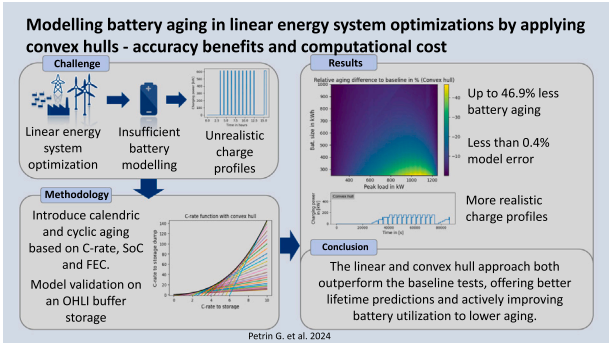

ARTICLE INFO

Keywords:
Energy system optimization
Battery aging
Oemof
Linear programming
Linear optimization
Convex hull
Overhead line islands
Aging model
LFP

ABSTRACT

Linear energy system optimization plays an important role in the design of future energy systems, due to its availability and low computational requirements. While linear optimization offers many benefits, the rise in popularity of battery storage and its use cases represents a challenge, commonly causing oversimplification by ignoring aging and its causes. Thus, this paper aims to include battery aging and subsequently battery optimized operation, to lower aging, into linear system optimization. Two approaches are highlighted, namely a basic linear aging implementation, as well as a convex hull approximation. These are then compared against the generic implementation found in oemof.solph, an open source energy modeling tool, to assess the benefits and drawbacks of including aging. The chosen case study for evaluation models a buffer storage for an overhead line island to reduce peak loads, enabling connections to weaker grids. The results show up to 46.9 % lower battery aging for the convex approach, compared to the generic baseline. Furthermore, the amount of aging is precisely determined by the convex approach, with errors below 0.4 % and the computational times close to the same magnitude, due to the lack of mixed integer linear programming. The suggested approaches of integrating battery aging into linear optimization should be integrated into future models to better predict and reduce battery lifetimes, allowing for better cost calculations in such systems.

1. Introduction

To decrease dependence on fossil fuels and lower emissions, the infrastructure, industrial and mobility sectors are transforming their systems towards electrified solutions and the optimized integration of renewable energy sources [1,2]. Yet, in order to ensure a successful transition either voluntarily or based on changing legislation [1,3],

* Corresponding author.
Email address: geert.petrin@dlr.de (G.K. Petrin).

https://doi.org/10.1016/j.apenergy.2025.126492
Received 9 April 2025; Received in revised form 13 June 2025; Accepted 15 July 2025
Available online 25 July 2025

efficient, reliable and cost-optimized systems are vital [3,4], for keeping energy prices low and maintaining competitiveness in the global market [3].

An important component of many new energy systems is battery storage. Due to the intermittency of renewable energy sources like wind and solar, they are used to buffer energy and provide more continuous power delivery [2,5,6]. Their scale of deployment varies significantly depending on the use case, ranging from small systems for residential PV storage or microgrids, to large-scale frequency reserves or renewable storage. Further use cases also include the better management of virtual power plants, peak load reduction, or the reduction of grid congestion [5,6]. Modern battery storage systems are mainly based on lithium ion batteries, given their high efficiency, energy density and cycle life. The widespread use of lithium-based solutions is underlined by the 77 % share of energy storage for grid stabilization they currently make up in the US [5]. The best lithium battery for stationary battery storage is the LFP battery, due to its high cycle life and relatively low cost [2].

Despite the widespread field of use for battery storages, one main drawback is the aging of batteries, over time and due to usage. Through the active usage of the battery and during idle, aging takes place as a result of chemical and physical processes like the formation of solid electrolyte interface (SEI) or dendrites within the battery [7,8]. While every type of battery has individual aging characteristics, all of them are influenced by external operating conditions like temperature, c-rate or depth of discharge [8–10]. As these parameters vary between every installation and use case, it is important to properly size and operate the battery storage, to inhibit premature failure and thus potentially high costs from replacement and downtime [7].

Despite declining battery costs [2], the aging effects of batteries, which are closely linked to the present operational conditions [10–12], are still an important factor in developing an energy system. Thus, many complex battery aging models have been created over the years trying to predict the aging behavior for different use cases [9–13]. However, despite the availability of aging models, the additional effort often leads to the neglect of aging, as shown by the many studies modeling energy systems without taking battery aging into consideration [7].

In order to optimize energy systems and batteries, linear programming can be a favorable approach due to its availability and simplicity. Through linearization, multiple energy types like gas, electricity and others can easily be combined and the computational effort remains low. These factors enable its widespread use in many fields of research, and especially in the energy segment the low computational effort of linear optimization can be used to perform design optimizations if wrapped in a non-linear external optimizer. This way, many different system combinations can be examined, offering a range of configurations to choose from.

Yet, due to its strictly linear nature, optimization can become problematic, as non-linear dependencies must be linearized for the model, introducing uncertainties [4]. Aging is highly nonlinear and thus efforts made include mixed integer programming (MILP) and/or decomposition methods to estimate depth of discharge (DoD) [7,14,15]. However, this greatly increases the computational effort, thus lowering reasonable timespans or temporal resolutions of the model [7], while also omitting other important aging factors. Since the convex hull approach can be realized in a purely linear fashion, it promises significant reductions in computational times compared to the mixed integer programming (MILP) methods.

This paper aims to introduce battery aging without the significant performance drawbacks of MILP by utilizing simple linear constraints creating a convex hull to describe the aging processes. Both calendric aging based on state of charge (SoC), as well as cyclic aging based on full equivalent cycles (FEC), are modeled by the aging model to not only measure aging but also to actively reduce it by optimizing said operating conditions, thereby reducing costs and emissions [2]. A simple linear and convex hull approach are compared against the generic storage component form the open energy modeling framework (oemof) to assess the benefits and drawbacks of each approach. oemof.solph [16] is a Python based open source tool capable of creating linear energy system models for optimization.

The test case applied to the model is a buffer storage used to reduce the impact of load spikes caused by an overhead line island (OHLI). OHLIs are short sections of overhead lines primarily located at train stations, where battery-electric multiple units (BEMU) can recharge their batteries during their stays at the station. As a result, the load profile includes spikes in power for short periods of time, while idling for the remaining time. The buffer storage is used to mitigate the peak loads experienced by the grid.

By presenting a new approach to battery aging in linear energy system optimization this paper contributes the following:

- Accurate battery aging within linear optimization based on calendric and cyclic aging.
- Active battery schedule optimization, reducing aging
- A strictly linear model without MILP, combining precision and low computational effort
- A flexible model structure, allowing for easy adoption of other battery models
- Implementation into an open source optimizer, based on a common platform to allow for more widespread usage

This paper is structured as follows: Section 2 introduces the aging mechanisms responsible for battery aging, as well as the utilized aging model. Section 3 then outlines the methodology of the different implementation approaches, explaining the integration of battery aging into the linear optimization. Section 4 presents the results of the case study, concerning peak load reduction for battery buffer storage systems in overhead line islands. Section 5 discusses the results. Finally, Section 6 states the conclusions.

2. Battery aging

The following sections introduce the mechanisms behind battery aging, the challenges of linearization and the chosen models, depicting the aging within this paper.

2.1. Battery aging mechanisms

Battery aging is a complicated process; thus, modeling is difficult due to the many different factors and subprocesses to consider. While differences between chemistries are expected, they also occur within the same chemistry resulting from packaging or manufacturing processes. Nonetheless, the main contributors to aging in lithium iron phosphate (LFP) cells are the loss of active material (LAM), the loss of lithium inventory (LLI) and lithium plating (Li plating). While all processes contribute to aging, the individual impact of each process is dependent on the operating conditions of the cell, where temperature, (dis)charge rate (c-rate), depth of discharge (DoD) and state of charge (SoC) represent the most important factors. Furthermore, aging is distinguished into cyclic and calendric aging, depending on whether it occurs during actively using the battery or in idle over time respectively [7].

LLI describes the loss of lithium through side reactions [17], with the formation of an SEI being the most prevalent side reaction. SEI forms when the electrolyte is in direct contact with lithium and acts as a protective layer around the anode. During cycling, this layer can crack, causing lithium dendrites to grow through the SEI, leading to the steady formation of new SEI. Thicker SEI layers in turn cause higher internal resistances and reduce the amount of available lithium, thereby lowering the battery's performance and capacity. SEI formation is the main overall cause of aging [8] and typically occurs at temperatures above 25 °C, high c-rates and high SoCs. LLI both causes calendric and cyclic aging [9].

LAM describes the loss of lithium by means of dendrites breaking of the anode, causing them to be electrically isolated and no longer usable. This so called “dead lithium” not only reduces the capacity of the battery but can also create safety concerns if it damages the separation layer within the battery. Similarly to LLI, LAM mainly occurs at elevated temperatures, high c-rates, high SoCs and long-term cycling [8–10].

Li plating only occurs during charging and describes the process where lithium ions do not properly intercalate into the graphite anode, causing an accumulation on the surface. Contrary to the other aging mechanisms, Li plating is reversible through discharging (lithium stripping (Li stripping)), yet the volumetric changes oftentimes accelerate the formation of SEI via cracking, which causes irreversible aging. Li plating predominantly occurs at high c-rates in combination with low temperatures. High SoCs and non-uniform charging can be contributingfactors as well [9].

2.2. Limitations of linear battery aging modeling

Next to the many interdependencies and aging processes, nearly all relations are non-linear [10,11,18], complicating their implementation into linear energy system optimization. As a result, not all relations can be properly modeled in oemof.solph. For example, DoD and temperature modeling is nearly impossible to model without binary variables, due to the difficulties in distinguishing between individual cycles or the non-uniform temperatures within the stacks. While the inability to model DoD is a drawback, the stationary nature of the examined storage allows for proper cooling and temperature management, reducing the need for a separate temperature model. Thus, the temperature for the battery is assumed to be constant at 25 °C. Factors like SoC or c-rates can be modeled and allow for the introduction of reducing capacities and end of life (EoL) conditions, where the battery can “break” during the optimization. The ability to model c-rates and SoC dependencies is valuable, since they are important factors, which can be influenced by adapting the operation schedule of the storage. Ideally, this causes the optimization to produce more realistic time series compared to the current generic approach. Since only the relations for c-rates and SoC are required, pseudo physical models, as often seen in literature [8,11,19], are most likely too complex and not of great benefit.

2.3. Literature model for linearization

The cyclic aging model used is proposed in [20], as it provides the desired parameters of the charge rate and energy throughput. The aging model proposed by Nakama et al. [20] contains two equations to calculate the aging in real time applications. The first function, shown in Eq. (1), computes the aging per timestep n. The second function in Eq. (2) calculates the total aging based on those individual aging steps:

$$Q_{\text{loss,n}} = (0.0032 \times \exp\left(-\frac{15161 - 1516 \times C_{\text{r,n}}}{R_{\text{g}} \times T_{\text{n}}}\right) \times (Ah_{\text{n}}^{Z}); Z = 0.824 \quad (1)$$

$$(Q_{\text{loss,total}})^{\frac{1}{Z}} = \sum (Q_{\text{loss,n}})^{\frac{1}{Z}} \quad (2)$$

where Q_{loss} is the capacity lost in %, Ah is the absolute amount of ampere hours passed through the battery, R_{g} is the gas constant and C_{r} is the c-rate. The temperature factor T_{n} is set to 25 °C in accordance with Section 2.2.

The cyclic aging model is used, to calculate the trajectory for varying c-rates, with Fig. 1 showing a selection of c-rates for an LFP storage capable of reaching 3500 full equivalent cycles (FECs) at 1C. The model is scaled to this representative cycle count based on the performed literature research [11,12,21].

The calendric model is taken from [13], as it provides aging based on temperature and SoC. For the calendar aging model parameterization, 16 cells were stored at different SoCs at each examined temperature (25, 40 and 50 °C). Periodically a checkup sequence consisting of two discharge charge cycles with pauses between each phase was performed. Unfortunately it is not exactly stated how often this checkup sequence was performed over the course of the experiment. Since multiple temperature levels are available in Keil et al. [13], the 25 °C data is being used for consistency. Fig. 2 shows the calendric aging over a timespan of nine months at 25 °C for different SoC levels.

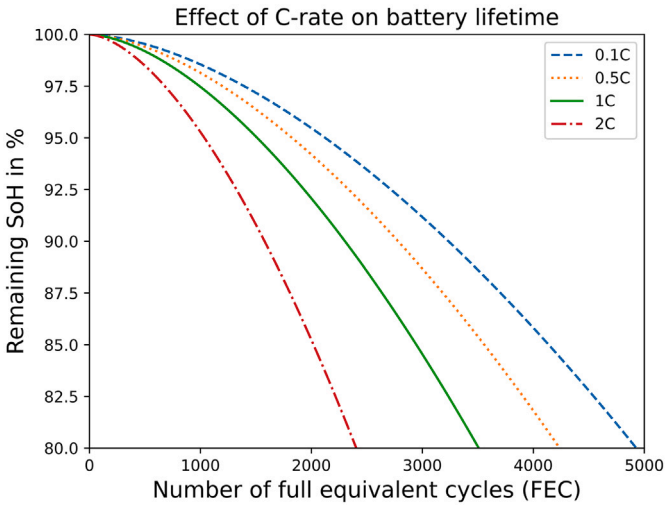

Fig. 1. Cyclic aging trajectories at different c-rates for the LFP storage at 25 °C [20].

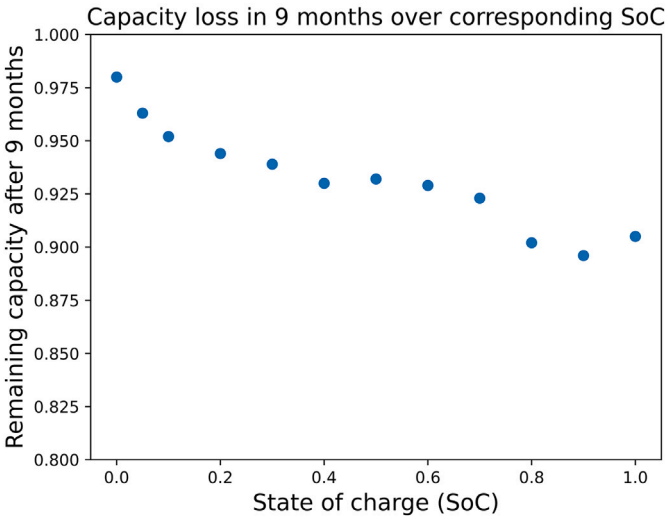

Fig. 2. Calendric aging for the LFP storage over 9 months at different state of charges and 25 °C [13].

3. Mathematical modeling

The modeling of the energy system is performed with oemof [22], by using its sub-package oemof.solph. oemof.solph offers the ability to create linear optimization problems based on energy systems and is available for Python. While other Python based solutions exist, many are based on Pyomo [23,24], including oemof, thus the findings in this paper are adaptable to other tools as well. The finished models shall be capable of calendric aging, capacity reduction and an end of life state for the linear model and additionally c-rate modeling for the convex model.

3.1. Modeling framework (oemof.solph)

oemof.solph [22] is a Python based tool for creating energy systems which can subsequently be optimized with solvers like CBC or SCIP. Within oemof.solph energy systems are made up of several different components, like converters, storage, or sources and sinks, which are interconnected through buses. Here, each connection between a bus and a component is realized as a so called flow, which can feature properties like costs, a maximum flow rate or fixed flows. An energy system must consist of at least one source, sink and bus, so that energy can enter, leave and flow through the system. Converters can be used to model technologies that interface with different energy types. For example, a CHP can be modeled as a Converter that converts the incoming fuel into heat and electricity at a certain efficiency. Generic storages can be used to store any kind of energy type, yet offer very little customization with respect to specific use cases like batteries or heat storage.

3.2. Generic model

The generic model consists of the available generic storage component provided by oemof.solph, as it is the default storage method within the toolbox. It offers some customization options like capacity, initial storage level, loss rate, in and outflow efficiencies, costs and maximum power, yet it is not capable of managing the charge and discharge processes beyond energy balancing. Thus, the storage does not differentiate between short high power bursts vs longer slower charging processes if the energy throughput is identical. As a result, erratic charging behavior with short charging spikes at full power, rather than slower charging over longer periods, is a common phenomenon with this type of storage implementation. Furthermore, it does not include any aging mechanisms, like capacity reduction or lifespan limitations. Despite these drawbacks, it is commonly utilized due to its simplicity and low computational cost. In this paper, it serves as the reference point of comparison, to evaluate the benefits of the linear and convex model.

3.3. Linear model

The linear aging model presented, adds calendric and cyclic aging, based on SoC and FEC respectively. It achieves this by combining multiple generic storage blocks and constraints with each other, which in combination act as one aging storage within the system. Its functionality is explained in depth in the following paragraphs.

The calendric aging of the storage is based on its SoC, at a temperature of 25 °C. Therefore a relation between lost capacity and SoC must be defined, which can be implemented into the model. This is done by a linear regression performed on the inverted data (e.g. loss of capacity instead of remaining capacity) from Fig. 2 [13]. The resulting function is shown in Eq. (3).

$$age_{\text{cal}} = 0.06931 \times SoC_{\text{s}} + 0.035131, \tag{3}$$

The next step involves the adaption of this relation to the model. Essentially a separate storage is added to the system, which counts up the aging over time. Thus the relation must be adapted to charge this storage each timestep according to the SoC. As the data in Fig. 2 is based on a 9 month period [13], and oemof operates on an hourly basis, the 9 months relate to 6570 h. By dividing Eq. (3) with 6570, the resulting Eq. (4) describes the amount of calendric aging per timestep ($age_{\text{cal,t}}$) in terms of the SoC (SoC_{s}).

$$age_{\text{cal,t}} = \frac{0.06931 \times SoC_{\text{s}} + 0.035131}{6570}, \tag{4}$$

To implement Eq. (4), the separate generic storage is added to the system, alongside a separate source and bus exclusively connected to the new storage. This storage of size 1 receives a constraint, which charges it every timestep based on the power defined in Eq. (4). The SoC of the second storage then represents the amount of lost capacity, with 0 being 0 % loss, 0.2 being 20 % loss (e.g. EoL) and 1 being 100 % loss. The SoC of the second storage is now used to constrain the maximum battery capacity of the actively cycled storage. A schematic, showing the new configuration is visible in Fig. 3.

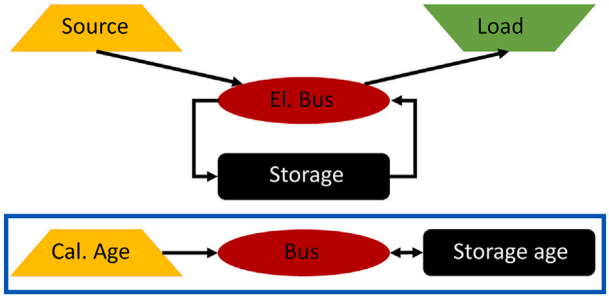

Fig. 3. Calendric aging addition (highlighted by blue surrounding) to an exemplary network.

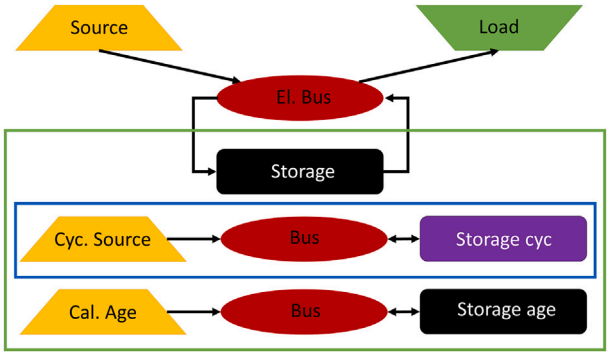

Fig. 4. Cyclic aging addition to an exemplary network, highlighted by the blue surrounding. The full linear battery system is indicated in green.

For cyclic aging, the same approach of a “counting” storage is used. Like for the calendric aging, a separate source, bus and generic storage are added to the system, to “count” the amount of occurred aging. The power flow into the new “counting” storage is now constrained by the inflow of the actively cycled storage, to store the amount of energy throughput the actively cycled storage experiences. Because the “counting” storage cannot discharge, this does not influence the overall energy balance of the system, while creating an end of life condition where the optimizer is stopped from further utilizing the battery when the counting storage is full. By now altering the counting storage’s size or the power relation to the cycled storage, virtually any lifespan in terms of full equivalent cycles can be set for the storage, causing the solver to utilize the battery more effectively if the EoL is reached within the simulation. During development, a 1:1 power relation between the actively cycled and “counting” storage at 1C has been used, so that the size of the “counting” storage can easily be mapped to the FEC at 1C. In addition to offering a predefined lifespan, the counting storage is, similar to the calendric aging, constrained to the cycled storage to reduce its available max. SoC with increased aging, simulating a linear decrease in state of health (SoH). A schematic, showing the full configuration is shown in Fig. 4.

3.4. Convex model

The linear model presents a first step into modeling battery aging, but as described in Section 2, the actual behavior is more intricate than the counting of full equivalent cycles. Thus, the convex model adds the ability to take different c-rates into account, since they represent an important factor for aging, as well as the operation schedule of a storage system. The modeling of the calendric aging remains unchanged from

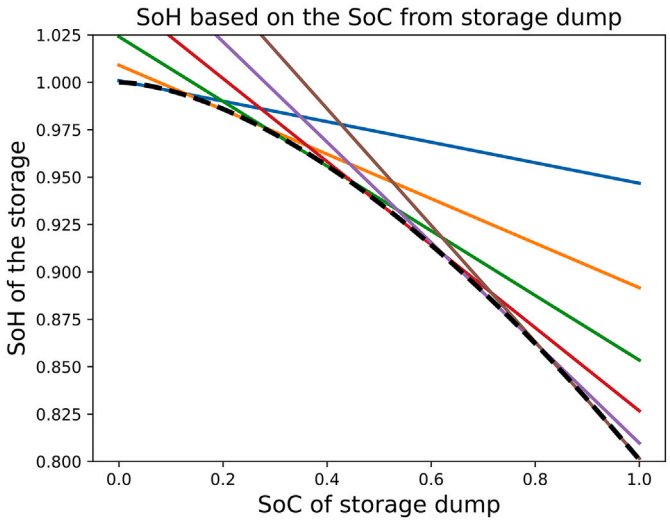

Fig. 5. Convex hull (colorful) representing the SoH relation (black) with 6 linear functions.

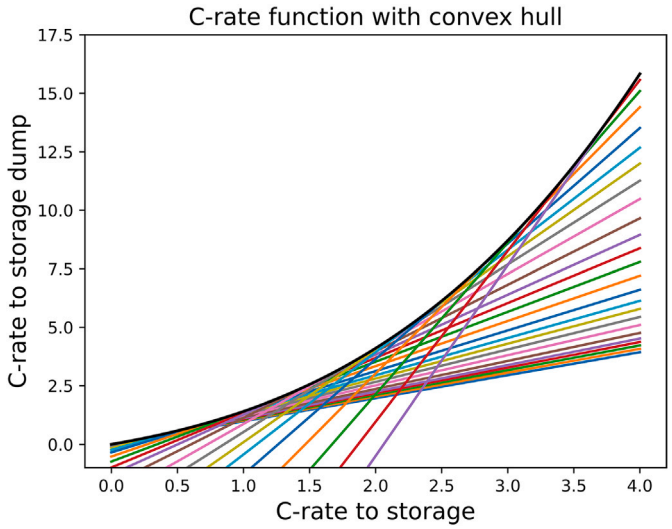

Fig. 6. Linear functions (colorful) of the c-rate convex hull against the theoretical function (black).

the linear implementation in Section 3.3. The main difference of the convex model is the constraints of the cyclic counting storage.

The aging model for both the capacity reduction and c-rate is based on [20] as shown in Eqs. (1) and (2) as well as Fig. 1. It is slightly adapted for implementation into oemof.solph. Initially, the aging trajectory until 80 % SoH is calculated and normed over a range between 0 and 1. This is done because the SoC of the "counting" storage is used to determine the amount of aging. A SoC of 1 represents the fully charged "counting" storage and thus the EoL state at 80 % SoH. 6 linear functions are fitted over said trajectory, creating a convex hull over the function. The result can be seen in Fig. 5.

For the c-rate-dependency, multiple trajectories at different c-rates are calculated (similar to Fig. 1) and their cycle count at 80 % SoH extracted. The cycle counts are then normed against the cycles reached at 0.1C, to obtain a factor (f_c), describing how much more aging occurs at higher c-rates (C_r) than 0.1C. Based on these factors, a quadratic regression is performed, yielding Eq. (5) with an R^2 value of 0.9999, indicating a near perfect fit:

$$f_c = 0.1026 \times C_r^2 + 0.3374 \times C_r + 0.9659 \tag{5}$$

This factor is essential for the c-rate implementation, as it describes how much faster the counting storage must be charged in comparison to the cycled storage, in order to achieve the desired aging effect. If the counting storage receives twice the power of the cycled one, it fills up twice as fast, effectively halfing the batteries lifespan. Since Eq. (5) only represents the factor between the charge rates for each storage, it must be multiplied by again by the c-rate going into the cycled storage ($C_{r,s}$) to receive the c-rate for the counting storage ($C_{r,c}$). This yields Eq. (6).

$$C_{r,c} = (0.1026 \times C_{r,s}^2 + 0.3374 \times C_{r,s} + 0.9659) \times C_{r,s} \tag{6}$$

Eq. (6) is then used to fit 30 linear functions between the range of 0 and 10C, to approximate the cubic behavior, as done for the capacity reduction above. This range is chosen for the model, because it remains within the empirical data for the cycling aging model ranging from 0.5C to 10C [25], while also allowing high power applications like the examined use case in Section 4. The following Fig. 6 shows the linear functions next to the theoretical one.

Upon generating the linear functions for the capacity reduction and c-rate dependencies, they are implemented by iteratively setting individual constraints for every linear function. As mentioned before, these constraints connect the inflow and outflow of the actively cycled storage to the "counting" storage used for the cyclic aging. For the capacity reduction every constraint is set as an upper limit, thus eliminating the necessity for binary variables while still approximating the model accurately. This is possible because the optimizer aims to utilize the full capacity of the battery when needed, consequently hitting the upper limit imposed by the capacity constraints. For the c-rate dependencies, the linear constraints are lower bounds, to approximate the nonlinear function. This works, since the counting storage has a price attached to its charging, thus causing the optimizer to favor the lowest possible charge rate limited by the constraints. The storage pricing is further discussed in the paragraph below. Noteworthy is, that the c-rate constraints are set twice, once for the charge and once for the discharge side.

Finally, the model must be calibrated to properly weigh the influence of the calendric aging and c-rate dependencies. If the model is not calibrated properly, either the influences of the c-rate or the calendric aging will predominantly determine the operation schedule, which might lead to sub-optimal results. The calibration can differ from case to case, and so it is performed on the study model used later, with the results shown in the results section. The factor described in the Section 4.2 represents that between the variable costs (cost per kWh of usage) for the counting storage of the calendric and cyclic aging. The costs associated with the counting storages per kWh of usage are at 0.1$/kWh, which at 3500 FEC translates to 350$/kWh investment costs. This data was taken from [26].

4. Case study

To validate the performance of the different approaches beyond synthetic tests, they are evaluated in a peak load optimization for an overhead line island (OHLI). OHLIs are short, electrified sections on non-electrified railroad tracks, designed to recharge battery powered trains during their stays at a station. As a result, their load profile contains many sharp power spikes, which only last for a few seconds or minutes and can exceed multiple megawatts. Battery buffer storage systems are one proposed solution to lower the effect of these load spikes on the grid connection point, yet their high investment cost calls for an optimized operation schedule and sizing to prolong their service lives and reduce costs. The used time series stems from a simulation performed on the railroad service between Zwiesel and Grafenau in Germany, with one BEMU serving this line. The maximum charging power is set to 1200 kW during standstill, according to EN50163 [27].

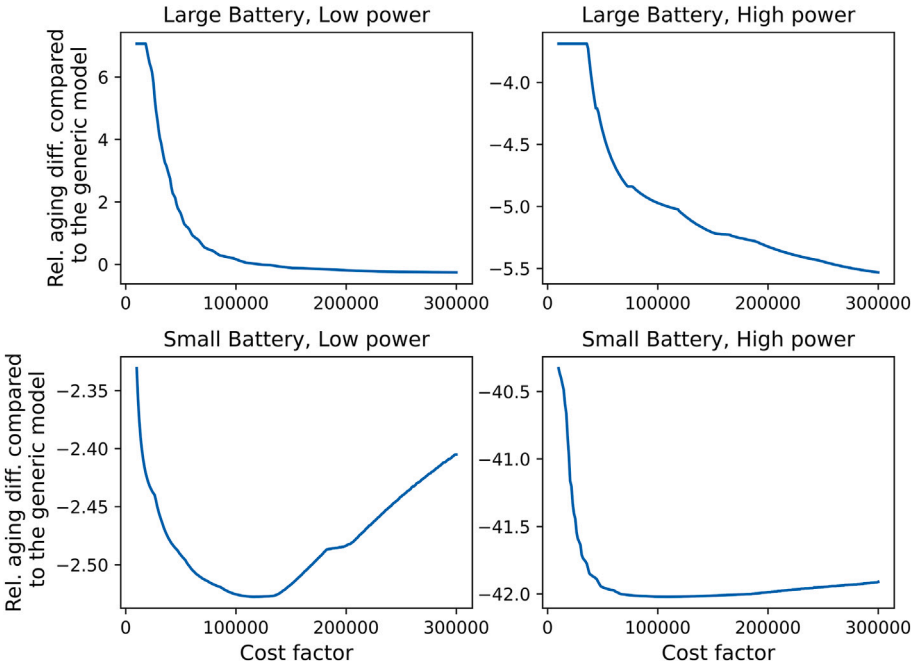

Fig. 7. Calibration of the cost factor between the calendric and cyclic aging.

4.1. Study model

The implementation of the case study into oemof utilizes essentially the same system presented in Fig. 4. The sink receives a fixed timeseries, represents the load of the OHLI, and the source with variable maximum power is the grid. The battery system is the only variable part between the approaches and is implemented as described in Sections 3.2–3.4 respectively. The only change made is within the linear system, at the power ratio between the cyclic counting storage and actively used storage. It is adjusted to 1:1.46 reflecting a charge rate of 2C based on the information from the aging model [20]. The battery cycle life for the linear and convex model is set to 3500 FEC at 1C, in accordance with the literature research performed [11,12,21] and the battery pricing remained at 350$/kWh [26].

The altered variables for this case study are the battery capacity and the maximum power available from the grid. The battery capacity ranges from 250 to 1800 kWh and the grid connection from 225 kW to 1250 kW. For both variables, 400 linearly spaced samples are taken, resulting in a 400 × 400 input matrix with a total of 160.000 samples. Through this method, the performance of the different modeling approaches across the entire reasonable configuration range is analyzed and compared. The baseline for comparison is given by the generic approach, since it is the standard method of implementing storage within oemof.solph. To analyze the aging performance and amount, the storage charge and discharge timeseries of each model are extracted from the results and the battery aging is calculated based on the model proposed in [13,20]. They can then be compared to the generic model's performance. The evaluation of the accuracy of the linear and convex models is done by comparing their aging based on the theoretical model, to the one recorded by their "counting" storages. This way the error in estimating aging can be determined.

4.2. Calibration

As mentioned in Section 3.4, the convex model must be calibrated to function properly. Visible in Fig. 7 is the preference for higher calendric costs with larger storage capacities, especially at low powers, while smaller storages present a minimum within the shown range.

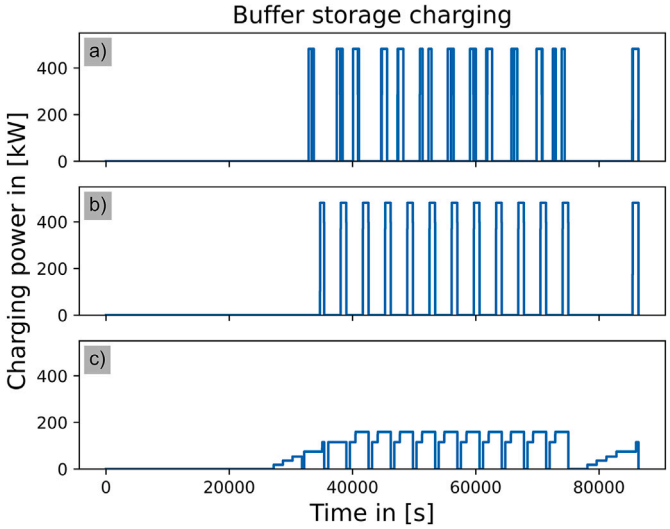

Fig. 8. Charging behavior of the different models at 250 kWh battery capacity and 500 kW grid connection, with (a) being generic, (b) linear and (c) convex.

For the remaining calculations, a factor of 145.000 is used, as it balances the different battery size requirements, providing the best overall performance.

4.3. Results

Fig. 8 shows the charging behavior of the battery storage for the three modeling approaches, with (a) being generic, (b) linear and (c) convex. The charging strategy for (a) and (b) is similar, featuring short charge intervals at maximum charge power just before the actual consumption of the OHLI. In contrast, the convex approach in Figure (c) charges at a more constant and significantly lower rate, with intermittent charge breaks at times when the battery is discharged.

Table 1 shows the calculation time averaged across the 160.000 samples from the case study for each approach. The computations are

Table 1
Avg. calculation time per sample.

	Generic	Linear	Convex
Avg. time in [s]	2.153	6.089	21.212
Std. derivation in [s]	0.1594	0.3010	1.3138

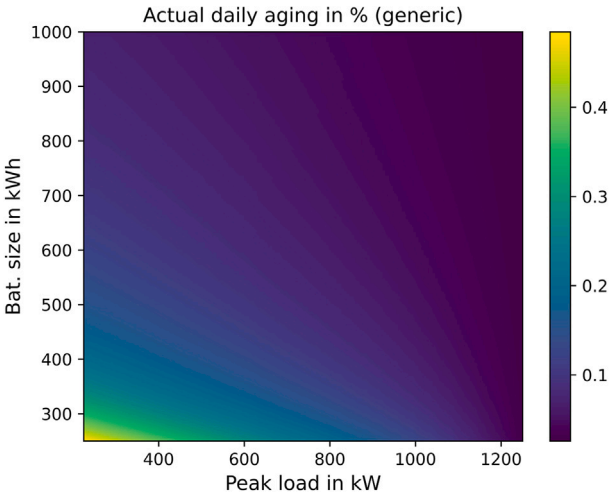

Fig. 9. Daily aging of the generic approach, based on the operation in %.

performed on a dual EPYC7542 system with 1024 GB of ECC DDR4 running at 3200 MHz. The system runs Ubuntu 20.04.6 LTS and 64 cores are assigned to the multiprocessing pool with a chunk-size of 500.

4.3.1. Generic model results

Fig. 9, shows the theoretical aging resulting from the operational schedule of the linear approach. The amount of aging increases with smaller battery sizes and grid connections, with the peak being reached at a 250 kWh battery size and 225 kW grid power, where 0.484 % aging occurs per day. Furthermore, a blue hue is visible across the left side of the figure, indicating that smaller grid connections, relate to more battery aging. The lowest amount of aging at the largest battery and grid connection is 0.026 %.

4.3.2. Linear model results

In Fig. 10, the difference in theoretical aging between the generic and linear approach can be seen. Most noticeable are the several areas and patches within the plot with hard borders and seemingly random placement. In addition to these areas, a regular pattern along the x-axis is visible with a repetitive rise and fall of battery life savings. Important to note is the reduction in battery aging across the entire solution space, peaking at around 2.3 %.

Fig. 11 shows the relative modeling error observed between the aging indicated by the linear model and the theoretical aging. The deviations between the generic and linear model range from $-25{,}5$ to $+45$ %. A battery size of 800–1000 kWh combined with a peak load below 300 kW results in the modeling errors above $+40$ %. The negative errors are observed primarily for battery sizes below 400 kWh. A narrow band across the plot is visible where the derivation is zero or close to it. Furthermore, vertical stripes at identical grid connections as in Fig. 10 are noticeable.

4.3.3. Convex model results

The convex approach yields significant battery aging reductions compared to the generic storage based model, as visible in Fig. 12. The entire solution space outperforms the generic model with up to 46.9 % less aging due to an improved operating schedule. In particular the range with high grid power and small batteries profits the most, with the highest

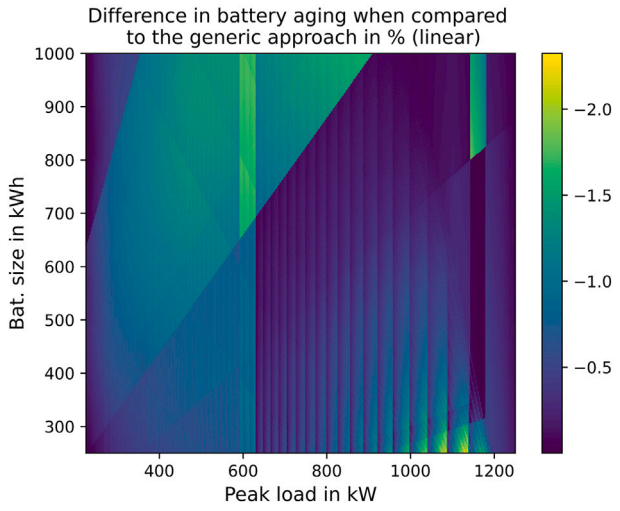

Fig. 10. Relative difference between the daily aging of the generic and linear approach.

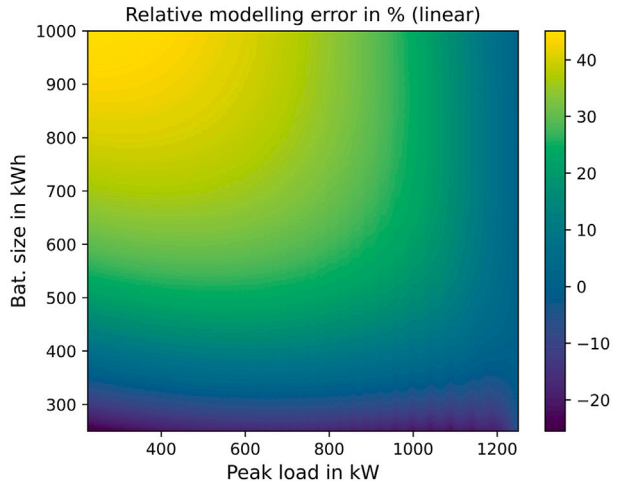

Fig. 11. Relative error between the aging indicated by the linear model and the theoretical aging according to the model.

reduction occurring at 250 kWh battery size and 1085 kW grid connection. Similar to the linear approach, vertical lines and patches are visible, although they are less pronounced.

In Fig. 13 the relative model derivation of the convex model is shown, featuring an alternating pattern with 19 valleys (blue) and 19 peaks (yellow/green). The individual lines appear linear and the magnitude of the peaks while overall reducing with increasing grid connection, are generally distinguishable into four main regions, each consisting of 5(4) lines. The overall relative error is at $+0.064$ to -0.36 %, which is significantly lower than in the linear approach.

5. Discussion

As shown by the simulations, up to 82 % peak load reduction is possible for the examined OHLI, with storage sizes as small as 250 kWh. Yet, at 0.42 % aging per day, such configurations experience fast aging due to discharge c-rates in excess of 4C and over 8.3 FEC per day. Low grid power, causing high discharge c-rates and battery cycling, are the main drivers of aging based on the light blue coloration across the left of Fig. 9. At 0.026 % per day, the lowest observed aging primarily stems

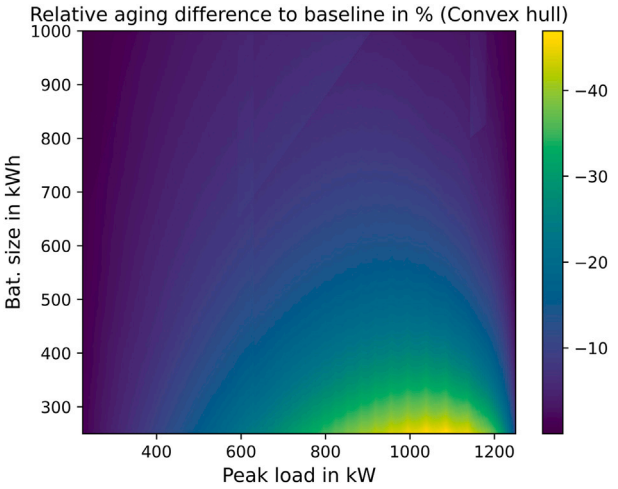

Fig. 12. Relative difference between the daily aging of the generic and convex approach.

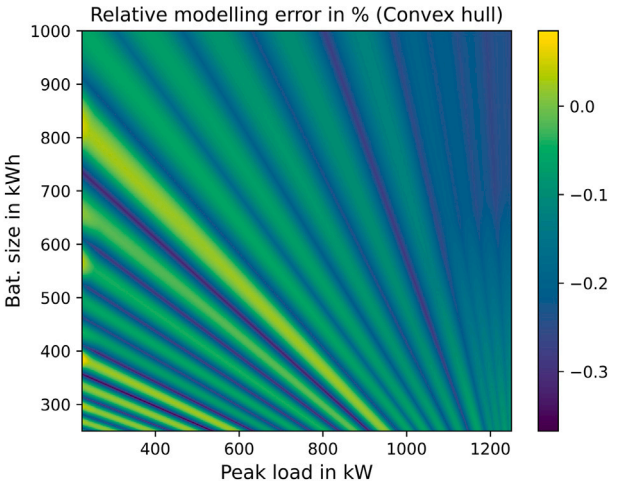

Fig. 13. Relative error between the aging indicated by the convex model and the theoretical aging according to the model.

from calendric aging and equates to a lifetime of around 10.5 years, being in line with shelf lives stated in literature [21].

Comparing the generic and linear approach in Fig. 10, the main benefit is the overall decrease in battery usage by up to 2.3 %. This results from implementing calendric aging and hence a preference for lower SoH states. In addition to the timing of charge processes, the overall charging profile remains mostly unchanged (Fig. 8a and b). Visually, the most distinct feature of Fig. 10 are the numerous areas and the repeating pattern along the x-axis, which can be attributed to the erratic behavior of the generic model. The pattern at the bottom results from the ability to charge up the storage in full power timesteps, with the green and yellow areas featuring non-full power timesteps, introducing variability and thus optimization potential. The other areas result from changing the charging times of the last charge process from 0 to 50 % SoC at the end of each simulation. If the timing aligns with the linear model, savings are lower, yet without a penalty in the generic approach, this timing can suddenly change at certain borders in the examined configuration space. These borders exist in Fig. 9, showing the generic aging, yet due to the scale of the heatmap they are not directly visible. Thus, the linear approach offers a more predictable optimized operation schedule albeit at around three times the computational cost. Due to the lack of c-rate dependent aging, the error in the counting storage determining the break condition and capacity reduction can be significant, as is visible in Fig. 11. Errors range from −25 to +45 %, resulting from the linear approximation of the cubic aging function. Subsequently, large batteries with low c-rates tend to age too fast, whereas small ones with high c-rates age too slowly. Accurate aging prediction is only present at the intersection point of the linear and cubic function at 2C, as well as the far-right area of the plot, where calendric aging takes over as the leading aging cause. The errors in aging prediction affect the lifespan and capacity reduction, yet due to the short time span of one day and thus the small amount of aging in the shown use case, they do not affect the results meaningfully. In longer simulations, they potentially become problematic if significant aging occurs during the simulation period. However, if typical c-rates are known previously to the simulation, the target c-rate of the model (in this case 2C) can be changed to better depict the aging behavior.

The convex approach is capable of reducing battery aging by up to 46.9 %, as visible in Fig. 12. Yet, it also increases computational time, requiring close to ten times longer than the generic approach (compare Table 1). In comparison to the model proposed in [7], which requires upward of 36,000 s without decomposition and around 1500 s with a two step decomposition to calculate 336 time steps, the convex approach still marks a significant improvement, taking only 20 s for 2880 timesteps. Other significant improvements are present at grid powers of between 800 and 1200 kW, with battery capacities of up to 500 kWh. At lower grid connections and larger batteries, improvements diminish, with the area of least improvement (below 0.5 %) ranging from 650 to 1000 kWh battery size at grid connections below 250 kW. The cause of this is the c-rate modeling function and the fixed output schedule of the batteries. At smaller grid connections, the c-rate on the charge side can reach maximum values of 0.225C, where the cubic function is still near linear. Furthermore, the discharge side experiences significantly higher c-rates, surpassing 4C for some cases, mainly contributing to the overall aging, which cannot be optimized by the model as it represents a fixed demand which must be fulfilled. Thus, the diminishing optimization potential on the charge side, with growing fixed aging on the discharge side, reduces the impact of the convex approach. Yet, the charging profiles of the convex approach, as visible in Fig. 8c, are beneficial beyond saving battery aging, representing more realistic behavior within an energy system. Furthermore, aging is well depicted in the convex approach, with maximum relative errors below 0.4 %, as seen in Fig. 13. The alternating stripe pattern visible stems from the convex hull approximation of the c-rate function, with each blue valley and yellow peak, representing one linear function. Upon closer inspection four individual regions can be made out, from 225 to 600 kW, 600 to 950 kW, 950 to 1150 kW and above 1150 kW. These regions each contain five yellow stripes (four for the rightmost one), aligning with the creation of the linear functions, which is done in unequally spaced five function blocks, to better represent low c-rate ranges. Of the 30 total functions describing the c-rate only 19 are visible in Fig. 13, showcasing the importance of simulation specific optimizations to increase accuracy or reduce computational effort by adjusting the number of functions and their covered span to the occurring demands. Like the linear model, the overall aging is very low for the examined case, so the capacity reduction is less impactful. More important is the parametrization concerning the degree of impact of the calendric aging. As visible in Fig. 7, this can significantly impact the model's performance in terms of operational strategy and thus the amount of aging it produces. Especially for large storage systems and low grid powers, c-rates are naturally low, so the additional calendric aging might outweigh the benefits created by the c-rate optimization. At a cost factor of 145,000 a good balance for this use case can be found, yet under different circumstances other parametrizations might deliver better results.

A potential drawback of the linear and convex models is the additional work required for parameterizing new battery types. This includes model research, fitting and constraint generation and validation.

However, if a pre-parameterized model is used, the implementation only varies slightly from the generic storage.

6. Conclusion

The generic approach to storage modeling offers an easy and fast way of including battery storage systems within energy system optimization, at the cost of functionality and realism. Both of these problems can be addressed by either the linear or convex models, enabling the introduction of aging, battery failures and capacity reduction. Furthermore they provide longer lifetimes due to optimized operation schedules. As shown by the case study, the convex approach is capable of precisely modeling aging and offering battery life savings of up to 46.9 %, with potentially even higher savings if the discharge side is flexible as well. While computation times are higher, they are magnitudes lower than those of existing approaches [7]. Furthermore, the convex battery modeling offers significant improvements in system modeling and design, as battery lifetime and pricing can be assessed more accurately and optimized beyond simple investment calculations. By altering the linear functions comprising the convex hulls, this approach can be fine-tuned to each application while modeling most battery types. Thus, the convex approach is beneficial to nearly all energy system optimizations containing battery storage systems, to achieve longer battery service life and more realistic operation. The linear approach can offer improvements for calendric aging next to delivering more predictable operation schedules. Due to its linear nature, modeling errors tend to be high unless typical c-rates are known previously and the model adjusted accordingly. For both approaches, the reducing capacity and battery failure are less important in the examined use case due to its short runtime and thus low overall amounts of aging, yet in longer optimizations their impact will increase. Nonetheless, the linear and especially the convex approach proved to be suitable methods for introducing battery aging in linear energy system optimization by including multiple aging mechanisms and effects. The convex approach in particular excels with its high accuracy and capability to greatly improve battery lifetime. Considering the long calculation times required and the simplifications performed in design optimization, the additional computational demands of the linear convex model could be problematic, despite the beneficial information they could deliver. Thus the main benefit of the linear and especially the convex approach is within operational scheduling and short term forecasting. Here overall system costs can be reduced by extending the battery lifetime and the more realistic charging profiles can be integrated into control mechanisms. Consequently, despite the potentially higher effort required for parametrization during the implementation and longer computation times, this approach should gain more widespread use, to better predict the energy systems of tomorrow due to its many benefits in modeling energy systems.

CRediT authorship contribution statement

Petrin Geert Kristian: Writing – original draft, Visualization, Software, Methodology, Formal Analysis, Conceptualization. **Arens Stefan:** Writing – review & editing, Supervision, Conceptualization. **Schoenfeld Patrik:** Supervision, Conceptualization. **Klement Peter:** Writing – review & editing, Supervision. **Schlüters Sunke:** Writing – review & editing, Supervision.

Declaration of competing interest

The authors declare the following financial interests/personal relationships that may be considered potential competing interests:

Geert Petrin reports that financial support was provided by Federal Ministry for Digital and Transport. Dr. Stefan Arens reports that financial support was provided by Federal Ministry for Digital and Transport. If there are other authors, they declare that they have no known competing financial interests or personal relationships that could have appeared to influence the work reported in this paper.

Acknowledgments

This work was carried out within the MOSENAS project, supported by the Bundesministerium für Digitales und Verkehr, grant number 03EMF0403B. The project MOSENAS is funded within the framework of the Federal Ministry for Digital and Transport's electromobility funding guidelines. Funding for this initiative is also provided as part of the German Recovery and Resilience Plan (DARP) via the European Recovery and Resilience Facilities (ARF) in the NextGenerationEU program. The funding guideline is coordinated by NOW GmbH and implemented by Project Management Jülich (PtJ).

Funded by:

Federal Ministry for Digital and Transport

Funded by the European Union NextGenerationEU

on the basis of a decision by the German Bundestag

Data availability

The authors do not have permission to share data.

References

[1] Chudy-Laskowska K, Pisula T. An analysis of the use of energy from conventional fossil fuels and green renewable energy in the context of the European union's planned energy transformation. Energies 2022;15(19):7369. https://doi.org/10.3390/en15197369

[2] Chen W-H, Hsieh I-YL. Techno-economic analysis of lithium-ion battery price reduction considering carbon footprint based on life cycle assessment. J Clean Prod 2023;425:139045. https://doi.org/10.1016/j.jclepro.2023.139045

[3] Jałowiec T, Wojtaszek H, Miciuła I. Analysis of the potential management of the low-carbon energy transformation by 2050. Energies 2022;15(7):2351. https://doi.org/10.3390/en15072351

[4] Klemm C, Vennemann P. Modeling and optimization of multi-energy systems in mixed-use districts: a review of existing methods and approaches. Renew Sustain Energy Rev 2021;135:110206. https://doi.org/10.1016/j.rser.2020.110206

[5] Chen T, Jin Y, Lv H, Yang A, Liu M, Chen B, et al. Applications of lithium-ion batteries in grid-scale energy storage systems. Trans Tianjin Univ 2020;26(3):208–17. https://doi.org/10.1007/s12209-020-00236-w

[6] Yang Y, Bremner S, Menictas C, Kay M. Modelling and optimal energy management for battery energy storage systems in renewable energy systems: a review. Renew Sustain Energy Rev 2022;167:112671. https://doi.org/10.1016/j.rser.2022.112671

[7] Maheshwari A, Paterakis NG, Santarelli M, Gibescu M. Optimizing the operation of energy storage using a non-linear lithium-ion battery degradation model. Appl Energy 2020;261:114360. https://doi.org/10.1016/j.apenergy.2019.114360

[8] Dessantis D, Di Prima P, Versaci D, Amici J, Francia C, Bodoardo S, et al. Aging of a lithium-metal/LFP cell: predictive model and experimental validation. Batteries 2023;9(3):146. https://doi.org/10.3390/batteries9030146

[9] Lin X, Khosravinia K, Hu X, Li J, Lu W. Lithium plating mechanism, detection, and mitigation in lithium-ion batteries. Prog Energy Combust Sci 2021;87:100953. https://doi.org/10.1016/j.pecs.2021.100953

[10] Petit M, Prada E, Sauvant-Moynot V. Development of an empirical aging model for Li-ion batteries and application to assess the impact of vehicle-to-grid strategies on battery lifetime. Appl Energy 2016;172:398–407. https://doi.org/10.1016/j.apenergy.2016.03.119

[11] Preger Y, Barkholtz HM, Fresquez A, Campbell DL, Juba BW, Romàn-Kustas J, et al. Degradation of commercial lithium-ion cells as a function of chemistry and cycling conditions. J Electrochem Soc 2020;167(12):120532. https://doi.org/10.1149/1945-7111/abae37

[12] Sanz-Gorrachategui I, Pastor-Flores P, Pajovic M, Wang Y, Orlik PV, Bernal-Ruiz C, et al. Remaining useful life estimation for LFP cells in second-life applications. IEEE Trans Instrum Meas 2021;70:1–10. https://doi.org/10.1109/TIM.2021.3055791

[13] Keil P, Schuster SF, Wilhelm J, Travi J, Hauser A, Karl RC, et al. Calendar aging of lithium-ion batteries. J Electrochem Soc 2016) A1872–A1880. doi:163(9). https://doi.org/10.1149/2.0411609jes

[14] Kazemi M, Zareipour H. Long-term scheduling of battery storage systems in energy and regulation markets considering battery's lifespan. IEEE Trans Smart Grid 2018;9(6):6840–9. https://doi.org/10.1109/TSG.2017.2724919

[15] He G, Chen Q, Kang C, Pinson P, Xia Q. Optimal bidding strategy of battery storage in power markets considering performance-based regulation and battery cycle life. IEEE Trans Smart Grid 2016;7(5):2359–67. https://doi.org/10.1109/TSG.2015.2424314

[16] Krien U, Schönfeldt P, Launer J, Hilpert S, Kaldemeyer C, Pleßmann G. Oemof. Solph—a model generator for linear and mixed-integer linear optimisation of energy systems. Softw Impacts 2020;6:100028. https://doi.org/10.1016/j.simpa.2020.100028

[17] Li B, Wang Y, Yang S. A material perspective of rechargeable metallic lithium anodes. Adv Energy Mater 2018;8(13). https://doi.org/10.1002/aenm.201702296
[18] Motapon SN, Lachance E, Dessaint L-A, Al-Haddad K. A generic cycle life model for lithium-ion batteries based on fatigue theory and equivalent cycle counting. IEEE Open J Ind Electron Soc 2020;1:207–17. https://doi.org/10.1109/OJIES.2020.3015396
[19] Schimpe M, von Kuepach ME, Naumann M, Hesse HC, Smith K, Jossen A. Comprehensive modeling of temperature-dependent degradation mechanisms in lithium iron phosphate batteries. J Electrochem Soc 2018;165(2):A181–93. https://doi.org/10.1149/2.1181714jes
[20] Nakama V, Lafoz M, Nájera J, Sal y Rosas D. Estimation of cycling aging of lithium-ion batteries for photovoltaic applications. J Phys Conf Ser 2022;2180(1):012011. https://doi.org/10.1088/1742-6596/2180/1/012011
[21] Porzio J, Scown CD. Life-cycle assessment considerations for batteries and battery materials. Adv Energy Mater 2021;11(33). https://doi.org/10.1002/aenm.202100771
[22] Hilpert S, Kaldemeyer C, Krien U, Günther S, Wingenbach C, Plessmann G. The open energy modelling framework (oemof) - a new approach to facilitate open science in energy system modelling. Energy Strategy Rev 2018;22:16–25. https://doi.org/10.1016/j.esr.2018.07.001
[23] Hart WE, Watson J-P, Woodruff DL. Pyomo: modeling and solving mathematical programs in python. Math Program Comput 2011;3(3):219–60. https://doi.org/10.1007/s12532-011-0026-8
[24] Bynum ML, Hackebeil GA, Hart WE, Laird CD, Nicholson BL, Siirola JD, et al. Pyomo - optimization modeling in Python. Springer eBook collection, vol. 67. 3rd ed. Cham: Springer; 2021. https://doi.org/10.1007/978-3-030-68928-5
[25] Wang J, Liu P, Hicks-Garner J, Sherman E, Soukiazian S, Verbrugge M, et al. Cycle-life model for graphite-lifepo4 cells. J Power Sources 2011;196(8):3942–8. https://doi.org/10.1016/j.jpowsour.2010.11.134
[26] Ayuso P, Beltran H, Segarra-Tamarit J, Pérez E. Optimized profitability of LFP and NMC li-ion batteries in residential pv applications. Math Comput Simulat 2021;183:97–115. https://doi.org/10.1016/j.matcom.2020.02.011
[27] Streuling C, Pagenkopf J, Schenker M, Lakeit K. Techno-economic assessment of battery electric trains and recharging infrastructure alternatives integrating adjacent renewable energy sources. Sustainability 2021;13(15):8234. https://doi.org/10.3390/su13158234